

First plasmas in the TJ-II flexible Heliac

C Alejaldre†, J Alonso†, L Almoguera†, E Ascasíbar†, A Baciero†, R Balbín†, M Blaumoser†, J Botija†, B Brañas†, E de la Cal†, A Cappa†, R Carrasco†, F Castejón†, J R Cepero†, C Cremy†, J Doncel†, C Dulya†, T Estrada†, A Fernández†, M Francés†, C Fuentes†, A García†, I García-Cortés†, J Guasp†, J Herranz†, C Hidalgo†, J A Jiménez†, I Kirpichev†, V Krivenski†, I Labrador†, F Lapayese†, K Likin†, M Liniers†, A López-Fraguas†, A López-Sánchez†, E de la Luna†, R Martín†, A Martínez†, M Medrano†, P Méndez†, K McCarthy†, F Medina†, B van Milligen†, M Ochando†, L Pacios†, I Pastor†, M.A Pedrosa†, A de la Peña†, A Portas†, J Qin†, L Rodríguez-Rodrigo†, A Salas†, E Sánchez†, J Sánchez†, F Tabarés†, D Tafalla†, V Tribaldos†, J Vega†, B Zurro†, D Akulina‡, O I Fedyanin‡, S Grebenschicov‡, N Kharchev‡, A Meshcheryakov‡, R Barth§, G van Dijk§, H van der Meiden§ and S Petrov||

† Asociación Euratom-Ciemat, 28040 Madrid, Spain

‡ General Physics Institute, Moscow, Russia

§ FOM-Instituut voor Plasmafysica 'Rijnhuizen', The Netherlands

|| Ioffe Physical Technical Institute, St Petersburg, Russia

Received 3 July 1998

Abstract. The first experimental campaign of the TJ-II stellarator has been conducted using electron cyclotron resonance heating ($f = 53.2$ GHz, $P_{\text{ECRH}} \approx 250$ kW) with a pulse length of $\Delta t \approx (80\text{--}200)$ ms. The flexibility of the device has been used to study five different configurations varying plasma volume and rotational transform. In this paper, the main results of this campaign are presented and, in particular, the influence of plasma-wall interaction phenomena on TJ-II confinement is briefly discussed.

1. Introduction

First plasmas have recently been achieved in the TJ-II stellarator using electron cyclotron resonance (ECRH) heating. TJ-II is a low magnetic shear stellarator of the Heliac type with an average major radius of 1.5 m and average minor radius ≤ 0.22 m. The magnetic field ($B_0 \leq 1.2$ T) is generated by a system of poloidal, toroidal and vertical field coils. The central conductors, which provide the flexibility of the TJ-II device (i.e. its rotational transform can be varied over a wide range), consist of a circular coil and two helical coils which are wrapped around the central conductor (figure 1). The main characteristics of TJ-II are: (a) strong helical variation of its magnetic axis; (b) very favourable magnetohydrodynamic (MHD) characteristics with potential for high beta operation; (c) flexibility in operation and (d) bean shaped plasma cross section [1]. The existence of closed and nested magnetic surfaces, in good agreement with the calculated ones, has been demonstrated in TJ-II by means of magnetic surface measurements carried out at low magnetic field [2]. Two gyrotrons (53.2 GHz, up to 700 kW) have been installed in the TJ-II stellarator. The first quasi-optical transmission

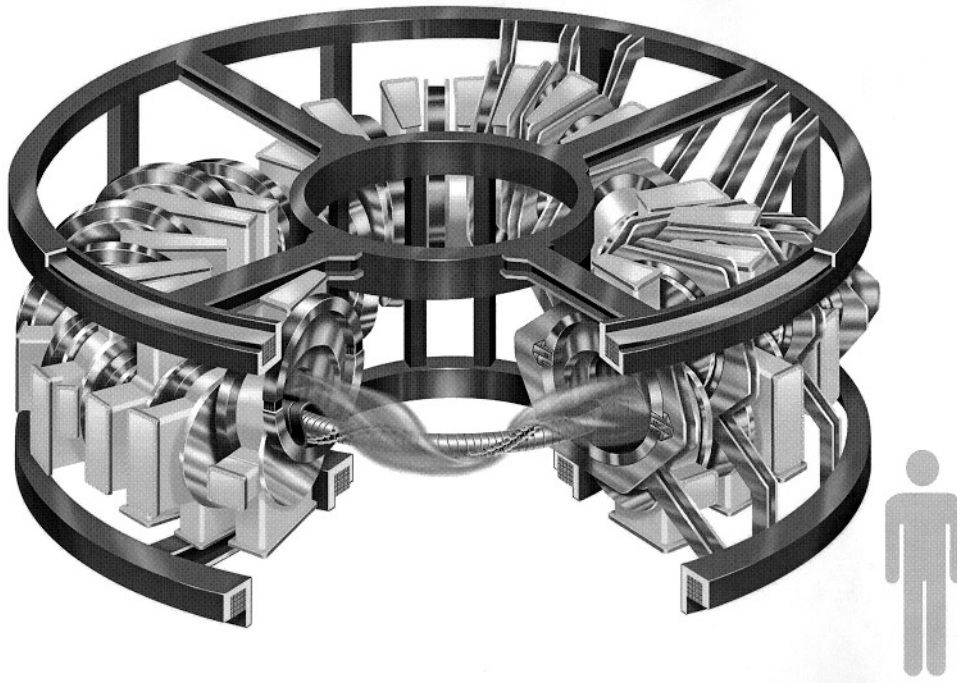


Figure 1. Schematic view of the TJ-II coil system.

line allows for perpendicular injection and the second one is equipped with a movable mirror located inside the vacuum chamber, thus providing the possibility of varying the location of power deposition as well as inducing current by electron cyclotron current drive (ECCD) [3, 4]. In a second stage, 2 MW of additional neutral beam injection (NBI) will be available at the end of 1999 [5]. A state of the art set of plasma diagnostics is being installed in the device. It includes most of the standard systems used in magnetic fusion experiments [6]. In addition, a powerful data acquisition system is in operation to handle the large amounts of data (≈ 125 Mb/discharge) [7]. The physics programme of the TJ-II stellarator is focused on transport studies in low collisionality plasmas, operational limits in high beta plasmas and on studies of confinement optimization and its relationship with the radial electric field.

2. Configurational effects and confinement studies in ECRH plasmas

2.1. Characteristics of the ECRH system

The first TJ-II plasmas were obtained using one gyrotron ($f = 53.2$ GHz, $P_{\text{ECRH}} \approx 250$ kW) with a pulse length of $\Delta t \approx (80-200)$ ms and with perpendicular injection into hydrogen plasmas. The gyrotron is fed by a high voltage power supply that is based on solid state commutative technology [8]. The ECRH output power, up to 300 kW, has a Gaussian-like beam shape. Power is launched into TJ-II plasmas through a boron nitride window mounted on the bottom port at the toroidal angle $\phi = 25^\circ$ perpendicular to the TJ-II magnetic field as extraordinary wave [9]. The transmission line consists of eight mirrors of which six cylindrical mirrors are coupled into pairs. The remaining two mirrors are elliptic. A receiving antenna is placed in the transmission line at the edge of the third mirror in order to monitor the microwave

power. A power transmission efficiency of 0.9 has been achieved along this mirror line and the wavebeam diameter is ~ 10 cm at the plasma border. In addition, a set of receiving antennae has been installed along the TJ-II vessel in order to measure the multi-pass absorption. The measurements show that the residual microwave power not directly absorbed by the plasma bulk is absorbed after a few passes through the plasma column. This is in agreement with the extensive linear ray tracing calculations carried out to analyse the performance of the ERCH system in TJ-II [3, 4].

2.2. Wall conditions

In the experiments reported here, only metallic (stainless steel) components have been exposed to the plasma. According to calculations and to magnetic field mappings (see later), the interaction between the plasma and the vacuum vessel is mainly located in the region surrounding the central coil system, i.e. in the groove. A set of stainless steel plates act as a thermal shield, thus creating an almost symmetrical toroidal limiter. Prior to experiments, vacuum levels of $\approx 1 \times 10^{-7}$ mbar are achieved using a set of turbomolecular pumps whose total pumping speed is ≈ 4000 l s $^{-1}$ [10]. Room temperature glow discharge cleaning with helium has been used for wall conditioning in the initial phase. In future phases, vacuum vessel baking (to 150°) and various coating techniques (such as boronization and lithiation) will be used [11]. The glow discharge is sustained at a voltage of ≈ 300 V (at 5×10^{-3} mbar) between the chamber and two L-shaped anodes. The total discharge current is typically 1 A per anode, equivalent to a current density of $4 \mu\text{A cm}^{-2}$. Two mobile limiters have been installed in TJ-II [12] to allow for interaction between the plasma and the vessel to be reduced when required. A set of Langmuir probes and thermoresistor are embedded in them to enable the scrape-off layer (SOL) region to be characterized. In the experiments presented in this paper, their overall limiting effect has been very low when compared to that of other parts of the TJ-II vessel.

2.3. Characteristics of the magnetic field

The parameters characterizing the five configurations considered in this study are shown in table 1. Figure 2 shows the vacuum flux surfaces at the toroidal angle $\phi = 0$ for three configurations. Free boundary equilibria were obtained using a three dimensional equilibrium code. Plasma configurations with a wide range of plasma volumes, 0.3–1.2 m 3 and an average plasma radius in the range 0.12–0.22 m have been chosen. The vacuum rotational transform profile is very flat ($\iota(0) - \iota(a) \approx 0.1$) and the magnetic well in the studied configurations is in the range (2–4)%. The poloidal location of the plasma–wall interaction in a specific interaction region evolves with the magnetic configurations. Although some degree of toroidal asymmetry is predicted by the calculations, no hot spots are foreseen in the groove area.

Table 1. TJ-II configuration characteristics. R_0 and R_b are the mod(B) ripple at the magnetic axis and at the boundary, respectively.

Name	ι_0	ι_b	Well (%)	Vol (m 3)	R_0 (%)	R_b (%)
38_38_37	1.50	1.62	2.6	0.337	3.0	18.4
46_46_43	1.60	1.73	4.0	0.560	2.3	24.2
100_32_60	1.42	1.52	2.2	0.934	1.5	32.0
100_40_63	1.51	1.61	2.3	1.065	1.7	35.8
100_50_65	1.61	1.73	2.7	1.260	2.4	40.7

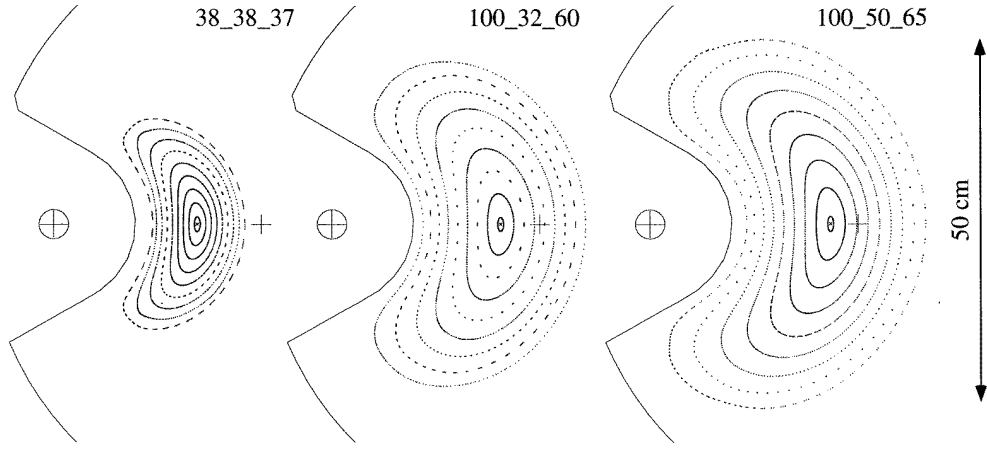


Figure 2. The vacuum configurations.

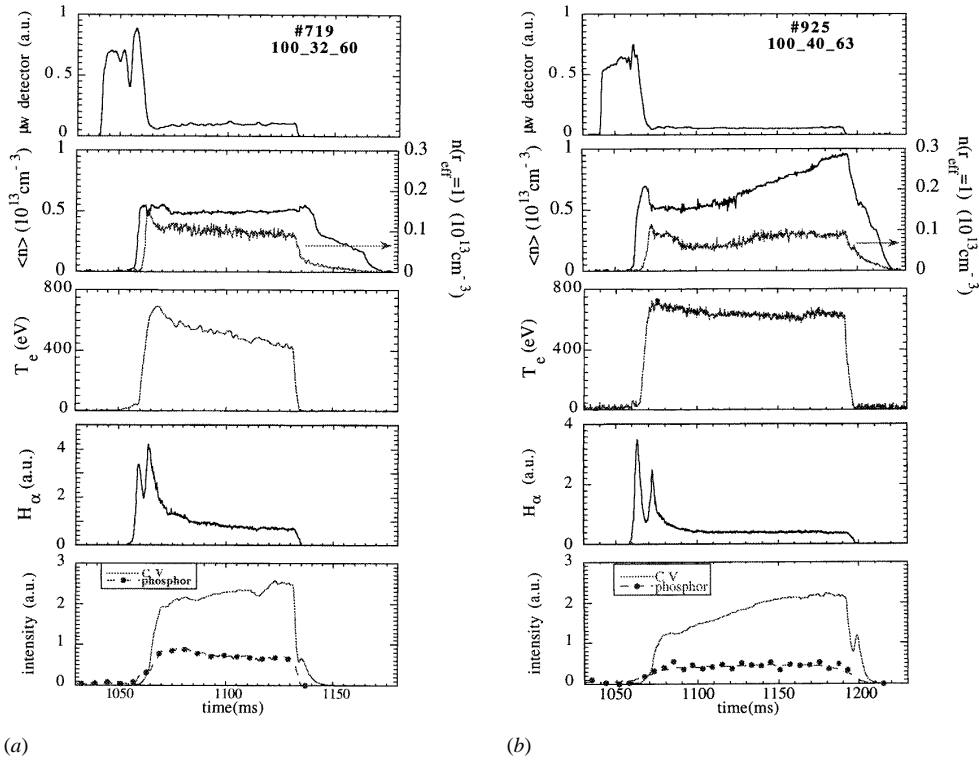
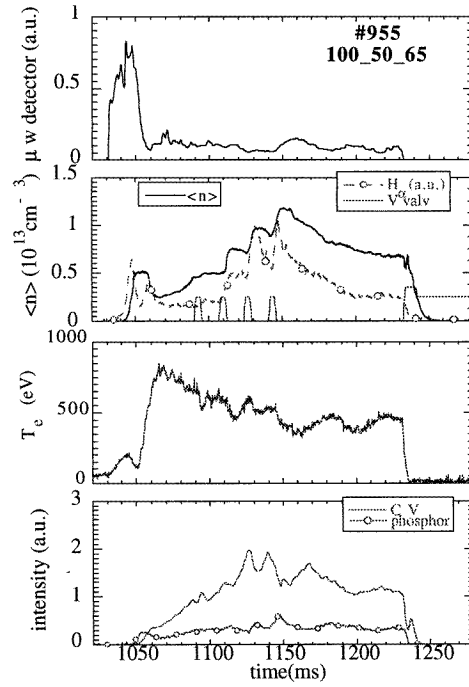


Figure 3. The time evolution of plasma parameters with (a) $\iota(0) \approx 1.42$, (b) $\iota(0) \approx 1.51$ and (c) $\iota(0) \approx 1.6$.

2.4. Confinement studies

The time evolution of ECRH discharges are shown in figure 3 for three magnetic configurations having central $\iota(0) \approx 1.42$, $\iota(0) \approx 1.51$ and $\iota(0) \approx 1.6$, respectively. Good conditions

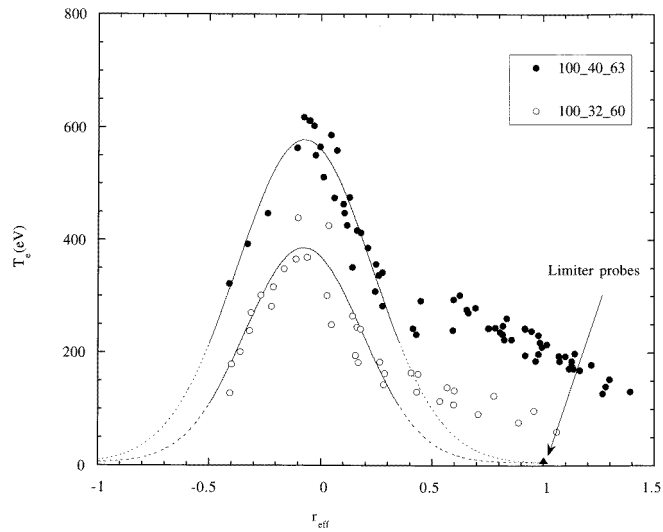


(c)

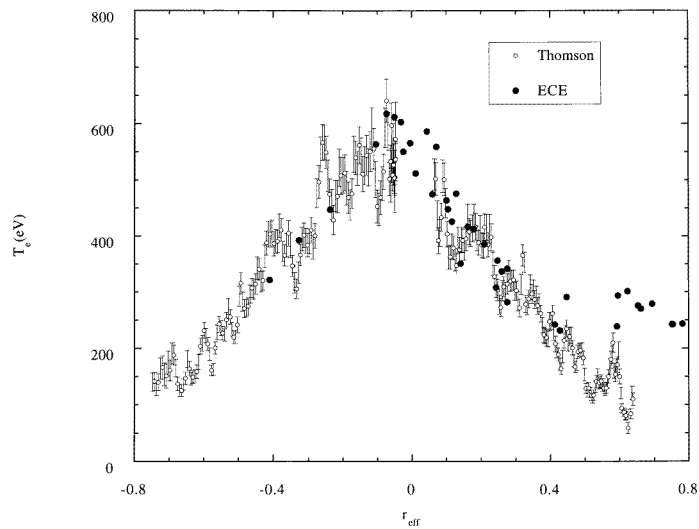
Figure 3. (Continued)

for pre-ionization and plasma start-up by ECRH were achieved by injection of hydrogen at several tens of milliseconds before the gyrotron pulse. Typical pressures are in the 10^{-5} mbar range, in agreement with particle balance and delays between the density built up and the gyrotron pulse are typically a few milliseconds. Quasi-stationary discharges with the ECRH lasting up to 200 ms were obtained. The average electron density obtained is of the order of $n_e \approx 0.5\text{--}1.0 \times 10^{19} \text{ m}^{-3}$ and central electron cyclotron emission (ECE) temperatures are in the range $T_e \approx (0.4\text{--}0.8) \text{ keV}$. Although the hydrogen is introduced in a short pulse before injection of the microwaves, a density plateau is usually obtained. The H_α signal decreases at the beginning of the plasma discharge whereas impurity monitors (i.e. C v) increase later. The corresponding electron temperature profiles obtained from second-harmonic ECE measurements are shown in figure 4(a). The peak ECE central temperatures for these discharges are 600 eV ($t \approx 1.51$) and 400 eV ($t \approx 1.41$). The distortion of the profiles on the low-energy side of the plasma is interpreted as being caused by a significant population of suprathermal electrons which gives rise to ECE at downshifted frequencies. The edge temperature obtained, from edge probes, are in the range, $T_e(a) \approx 10\text{--}20 \text{ eV}$. A preliminary comparison between ECE and first multiposition Thomson scattering measurements shows an excellent agreement, as can be seen in figure 4(b). Plasma currents in the range of $I \approx 0.5 \text{ kA}$ have been measured, which appear to depend on the location of the plasma resonance (on/off axis heating) consistent with electron cyclotron current drive (ECCD) calculations.

The fast decay of the H_α signal is consistent with the low recycling expected for He conditioned metallic walls. The constant electron density at longer times implies the presence of impurities as fuelling species. The progressive change in plasma composition is confirmed by charge exchanged neutral fluxes which decrease strongly with the H_α signal.



(a)



(b)

Figure 4. (a) Electron temperature profiles obtained from second-harmonic ECE measurements for the discharge series with $t(0) \approx 1.42$ and $t(0) \approx 1.065$. The maximum that appears on the low-field side of both profiles is due to the presence of a suprathermal electron population. Also shown is the edge temperature measured with the Langmuir probes installed in the limiter. (b) Comparison between ECE and Thomson scattering measurements; Thomson data are obtained in a single shot.

In addition, higher edge temperatures are observed during the initial, cleaner phase. Analysis of spectroscopic data is currently in progress to quantify carbon, nitrogen, oxygen and metallic impurity concentrations. Evidence for important wall effects occurring during this initial experimental phase is also provided by mass spectrometric data. The release of He, that has been implanted in the metal walls during the overnight glow discharge conditioning, after each plasma shot is plotted in figure 5 for a typical operating day. A systematic decrease of

total desorbed He per shot can be clearly seen. Lower values were systematically detected for short plasmas or cold ones. Conversely, higher values are associated with shots having x-ray (HXR) production. The initial values of desorbed He, as indicated by an absolutely calibrated differentially pumped mass spectrometer, correspond to the observed density increase during the first shots after glow discharge, assuming that He is completely recycled. Spectroscopic data (the He I line) are in good qualitative agreement. Results for different configurations indicate an impurity dilution effect as the ratio of plasma volume to plasma-surface interaction increases.

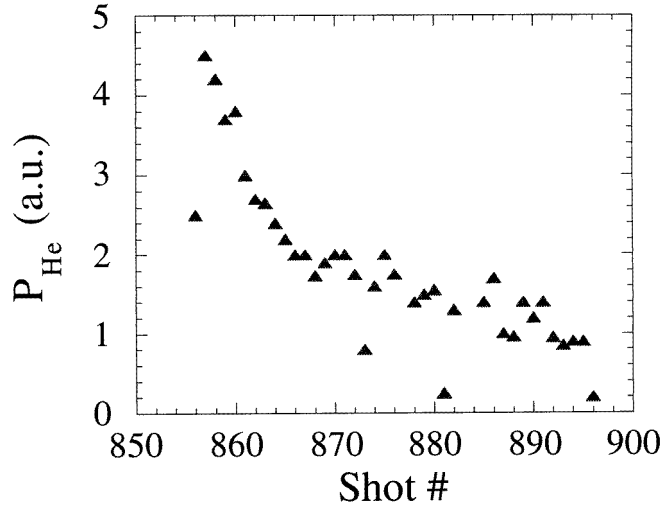


Figure 5. Mass spectrometric signal of total He release during each plasma shot. The evolution during the working day is shown.

In configurations with the largest volumes ($V \approx 1.2 \text{ m}^3$), plasma densities up to the cut-off density ($n_e(0) = 1.75 \times 10^{19} \text{ m}^{-3}$) have been obtained with appropriate gas puffing during the plasma discharge (see figure 3(c)). In general, the use of external fuelling was particularly successful in obtaining increased densities in initial shots made after conditioning, this being concurrent with best wall conditions. The time decay of the H_α signal indicates effective particle confinement times of $\tau_p^* < 15 \text{ ms}$ for the wall conditions reported here.

Global confinement properties have been found to be strongly dependent on plasma volume. Figure 6 shows stored plasma energy against plasma volume. The stored energy increases from 200 J, in the smallest plasma configuration ($V \approx 0.34 \text{ m}^{-3}$), to above 1 kJ, in the plasma configuration with $V \approx 1.2 \text{ m}^{-3}$. In the largest plasma configurations, which have a line-averaged density $n_e \approx 0.5 \times 10^{19} \text{ m}^{-3}$, the measured stored plasma energy, W , is $\approx 1 \text{ kJ}$ and the global energy confinement time $\tau_E^* = W/P_{\text{ECRH}} \approx 4 \text{ ms}$.

In TJ-II, the main accelerating electric field is induced by the ramping of currents in circular and helical coils. During initial TJ-II discharges, HXR generated by fast electrons have been measured using NaI detectors during the ramp-up, flattop and ramp-down phases of the coil currents. Furthermore, photons that had energies greater than 100 keV, thus being created within a few milliseconds of the existence of the electric fields, have been detected. In order to reduce the generation of runaway electrons, a mechanical shutter has been installed. It consists of a pneumatically operated paddle that is swept through the poloidal magnetic surfaces in a few milliseconds both before and after the flattop, thus intercepting electrons

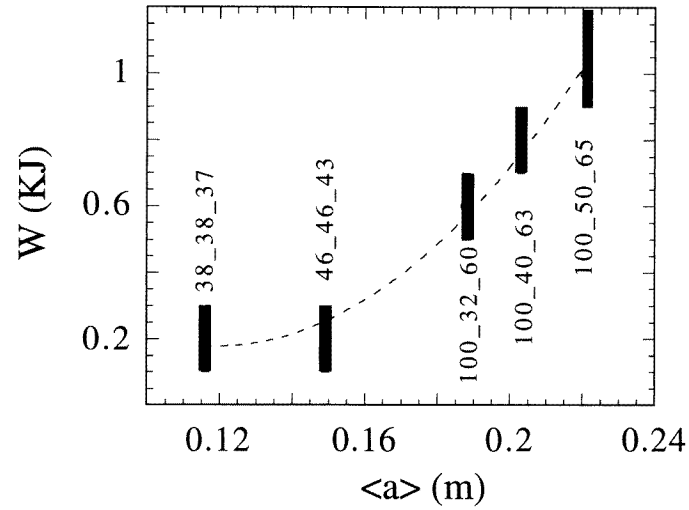


Figure 6. Stored energy against plasma volume.

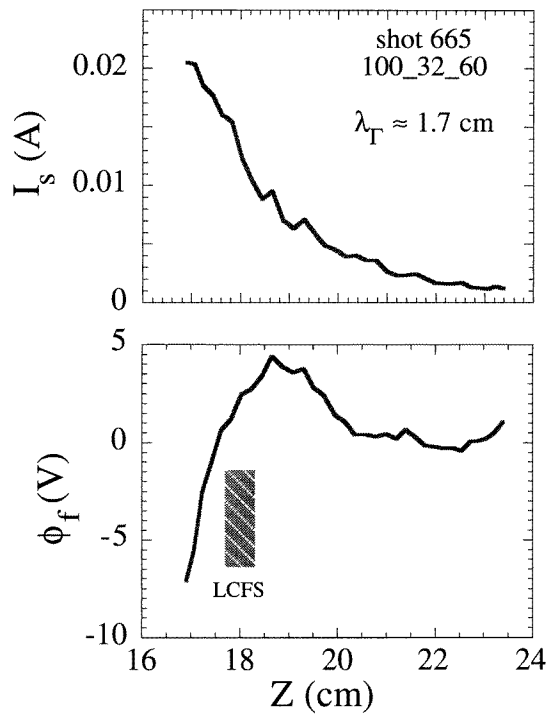


Figure 7. Radial profiles of the ion saturation current and floating potential. The LCFS position deduced from equilibrium codes is very close to the location where the floating potential reaches its maximum value. Z refers to the probe position related to the device equatorial plane.

associated with the magnetic field lines over the whole cross section. Initial experiments have shown efficient suppression of these electrons [13].

2.5. Plasma edge studies

The radial profile of plasma parameters has been investigated in the plasma boundary region for different plasma configurations by means of fast movable probes and probes installed in movable poloidal limiters. In general, good agreement (within ± 0.5 cm) has been obtained between the location of the last closed flux surface (LCFS) computed from equilibrium codes and the confinement plasma radius (defined as the point where the electric field changes direction from positive (radially outwards) to negative (figure 7)). The presence of the natural 8/5 rational surface in the plasma boundary region, predicted by equilibrium codes for this configuration, is clearly seen as a flattening in the edge profiles (i.e. ion saturation current and floating potential), see figure 8. First measurements of plasma fluctuations have been carried out at the plasma

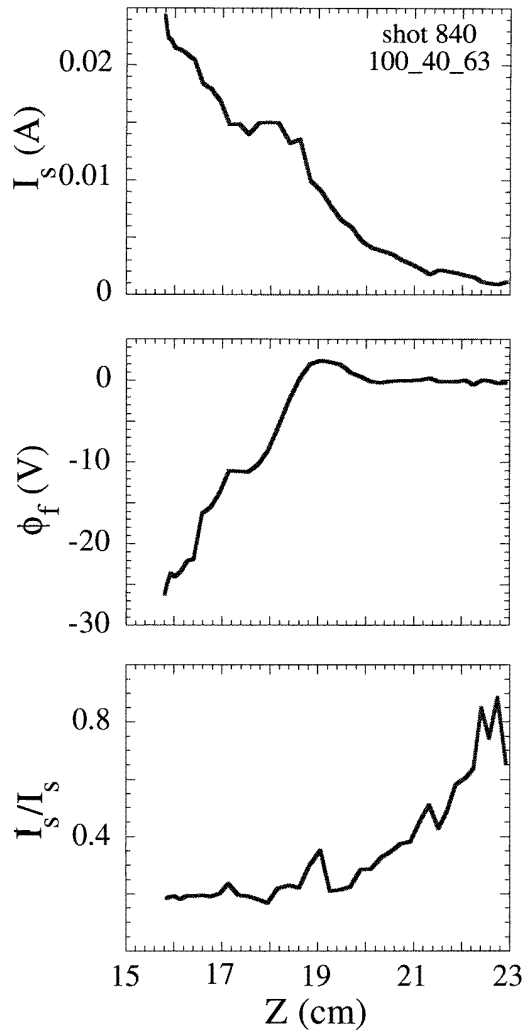


Figure 8. Radial profiles of ion saturation and floating potential together with normalized ion saturation current fluctuations in the plasma configuration for $\iota(0) \approx 1.5$. The flattening of the profile in the plasma boundary region is interpreted in terms of the influence of magnetic islands (8/5) in plasma profiles.

boundary region. The normalized level of ion saturation fluctuations is about 20% at the LCFS.

By considering that all losses are due to the limiter while assuming that other sources or sinks can be ignored, the radial flux is given by $\Gamma_{\text{LCFS}} \approx 0.5n(a)c_s\lambda/L_c$, L_c being the characteristic connection length to the limiter and λ the e-folding length of the particle flux. Field mapping calculations yield $L_c \approx (4-5)$ m and probe measurements indicate $\lambda \approx 1.5-2$ cm at the top region of the plasma bean shaped region (toroidal angle, $\phi = 38$). The diffusion coefficient is therefore $D_{\text{SOL}} = \Gamma_{\text{LCFS}}/\nabla n \approx 1 \text{ m}^2 \text{ s}^{-1}$. This value is close to D_{Bohm} . A rough estimate of the global particle confinement time is given by $Vn_e/S\Gamma_{\text{LCFS}}$, S being the plasma surface and V the volume. This ratio is in the range 5–8 ms.

3. Conclusions

The first plasmas of the TJ-II stellarator have been successfully achieved using a 53.2 GHz gyrotron with ECRH ($P_{\text{ECRH}} \approx 250$ kW). Quasi-stationary discharges lasting up to 200 ms have been obtained with central electron temperatures from 400 to 800 eV, plasma densities $n_e \approx (0.5-1.75) \times 10^{19} \text{ m}^{-3}$, stored energies in the range 0.2 to 1 kJ and global energy confinement times of up to 4 ms. As expected, in TJ-II, the plasma-wall interaction shows very distinctive features that play an important role in machine operation. An intense programme in first wall conditioning is under development to control the influence of neutrals and radiation on plasma properties.

References

- [1] Alejaldre C et al 1990 *Fusion Technol.* **17** 131
- [2] Ascasibar E et al 1998 *J. Plasma Fusion Res.* **1** 183
- [3] Castejón F, Alejaldre C and Coarasa J A 1992 *Phys. Fluids B* **4** 3689.
- [4] Tribaldos V, Jiménez J A, Guasp J and van Milligen B Ph 1998 *Plasma Phys. Control. Fusion* **40** 2113
- [5] Guasp J, Liniers M, Fuentes C and Barrera G 1999 *Fusion Technol.* at press
- [6] Sánchez J et al 1998 *J. Plasma Fusion Res.* **1** 338
- [7] Vega J, Crémy C, Sánchez E and Portas A *Fusion Eng. Design* at press
- [8] Martin R et al 1992 *Proc. 17th SOFT. (Rome, Italy)* p 897
- [9] Sorolla M et al 1997 *Int. J. Infrared Millimeter Waves* **18** 1161
- [10] Tabarés F L et al 1994 *Vacuum* **45** 1059
- [11] Tabarés F L et al 1999 *Proc. 13th PSI Conf. (San Diego 1998) J. Nucl. Mater.* at press
- [12] de la Cal E et al 1999 *Proc. 13th PSI Conf. (San Diego 1998) J. Nucl. Mater.* at press
- [13] Rodríguez L et al 1998 *Rev. Sci. Instrum.* **70** 645